MULTIPHASE EXPLOSIONS ON MARS: NUMERICAL STUDIES OF PHREATOMAGMATIC BLAST DYNAMICS J. Dufek[1] , J. Telling[1], M. Manga[2], [1]School of Earth and Atmospheric Science, Georgia Institute of Technology, Atlanta, GA 30332 (dufek@gatech.edu), [2] Department of Earth and Planetary Science, University of California, Berkeley.

Introduction: Phreatomagmatic activity may have helped shape the surface of early Mars and the landforms generated in such events provides clues to both the magmatic and environmental conditions in the near surface. We study the dynamics of explosions generated by rapid steam generation in the near surface when magma intersects a source of liquid water or ice. Using an EEL multiphase model we study the thermal evolution in the source region, the pressure evolution due to phase change, and the compressible multiphase dynamics of the blast and subsequent gravity currents. This numerical model was validated on similar blast conditions through a sequence of scaled analogue experiments. Both the dilute and dense part of the granular flow are modeled and we correlate dynamics during the blast to eventual depositional features such as grain size sorting, flow runout, crater size and shape, and distribution of large clasts. In this way we correlate the pre-eruptive conditions to landform morphology that may be useful in interpreting on-going observations. We also report on the mixing of gas species in explosive events to better understand the distribution of water during and after the blast. Using microsphysical models we also assess the spatial and temporal potential for electrostatic and hydrous particle aggregation.

Multiphase Numerical Approach: In order to study phreatomagmatic blasts and subsequent particle-laden gravity currents (base surges), which are heterogeneous, compressible, and time-dependent flows, we use an Eulerian-Eulerian-Lagrangian (EEL) approach [1]. This model will predict grain size distributions and deposit thickness variation with distance from the source given variable Martian atmospheric conditions, thus providing a quantitative way to assess various features and their relationship with past climates on Mars. Separate continua are used to model both the gas and particle phases, similar to other multiphase modeling approaches [2-5]. In the multicontinua (Eulerian-Eulerian) approach, each particle phase and the carrier fluid phase have separate conservation equations for mass, momentum, and energy, along with drag coupling between phases. Additionally, if phase change occurs, such as the production of steam, there is also be a conservation of mass coupling. The stress tensor reflects the interaction of particles with each other, internal to each phase [6-8] The numerical approach has been adapted from the MFIX (multiphase flow with interphase exchanges) model developed by the Department of Energy[9].

Comparison with Experiments: Comparison with two suites of experiments were used to validate the granular explosions in the numerical work. We examined the eruption of an over-pressurized lens of gas using scaled laboratory experiments. Modifying a previously designed and built apparatus [10] we released a pressurize gas lens beneath a bed of fine grained ballotini (40 microns). The upper reservoir of the apparatus is attached to a vacuum pump and we can reduce its pressure to a specified value. Both the upper reservoir and the high pressure lens are monitored by high frequency pressure transducers so we can monitor the initial pressure and pressure evolution during the experiment. During the experiment we use the portals in the upper reservoir to image the experiment using high-speed video (at up to 2000 frames per second). The pressurized lens of gas is initially contained beneath a mylar diaphragm; surrounding the top portion of the diaphragm is a resistance heating wire. When we have achieved the desired pressures, we then provide electricity to this circuit and the wire heats up sufficiently to weaken the mylar and initiate the blast (Figure 1). We use electricity to rupture the mylar to both insure a highly controlled pressure environment at blast initiation, but also to insure reproducibility in failure of the diaphragm. The final deposit morphology is measured using a laser photogrammetry technique[11]. With these controlled conditions we were able to perform simulations with identical conditions comparing crater morphology and the dynamics of blast (Figure 1). We performed a similar comparison with the experiments of Ross et al.[12] in which a pressurized jet of gas in roughly 2D geometry is injected in a granular bed.

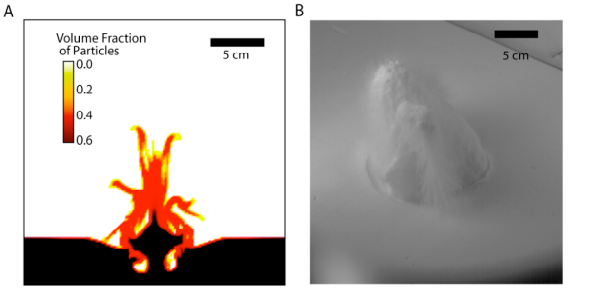

Figure 1: Comparison between numerical simulations and experiments. Panel A shows a cross section of the volume fraction of particles ~0.1 seconds after the initiation of the blast. Panel B depicts an experiment using the same conditions in A (1 atm pressure, 2 atm over-pressure), also at approximately ~0.1 s after blast initiation. In both cases the blast excavates the crater and generates fine particle-laden gravity currents that form a surrounding apron.

Comparison of Eruptive Morphology at Different Atmospheric Pressures: The average flow features, crater morphology and blast heights in the small scale experiments and in the numerical simulations matched well for both sets of experiments, although instantaneous variations of the granular explosion varied due to sensitivity to initial conditions. Crater morphology was found to be relatively insensitive to atmospheric pressure conditions in contrast with the height and morphology of the base surge which was very sensitive to atmospheric conditions.

We explored large scale features by conducting 2D and 3D simulations varying the atmospheric pressures. In these simulations a high pressure water vapor lens initiates the explosion into a carbon dioxide atmosphere. Similar to the small scale findings, the crater morphology was determined by source conditions (gas lens shape, depth and pressure). The base surge morphology depended primarily on atmospheric pressure with intial pyroclastic density currents heights 4-10 times larger at 10^3 Pa compared to 10^5 Pa atmospheric pressure. Likewise ballistic impact energies were over two orders of magnitude larger for the low pressure conditions. However, entrainment was less efficient under low pressure conditions producing less vigorous mixing via kelvin-helmholtz instabilities and resulting in longer runout.

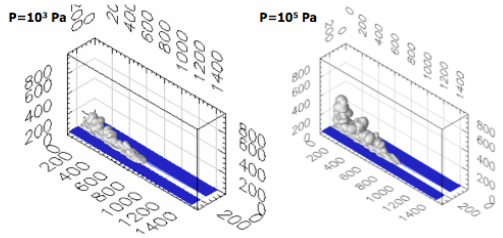

Figure 2. 3D simulations of pyroclastic density currents for 10^3 and 10^5 Pa atmospheric pressure. Shown is the isosurface of 10^{-5} volume fraction of particles.

Accretionary Lapilli Formation Potential: Accretionary lapilli consisting of aggregated ash particles are commonly observed in terrestrial phreatic events. Three primary factors are necessary for their formation: 1. Condensing water vapor, 2. Abundant particle-particle collisions, and 3. Low energy collisions [13]. We explored the conditions necessary for accretionary lapilli formation under different potential atmospheric conditions numerically and also conducted experiments to determine the aggregation efficiency. Figure 3 shows the mass fraction of water vapor in an evolving eruption into a 10^3 Pa carbon dioxide atmosphere. Due to the abundant water vapor driving the blast and decompression of the vapor, a significant fraction of the particle rich region reaches saturation. Using kinetic theory we determined that under most atmospheric conditions accretionary lapilli formation is expected with aggregation focused on the margins of the expanding blast and in the head and kelvin-helmholtz mixing zones in the base surge.

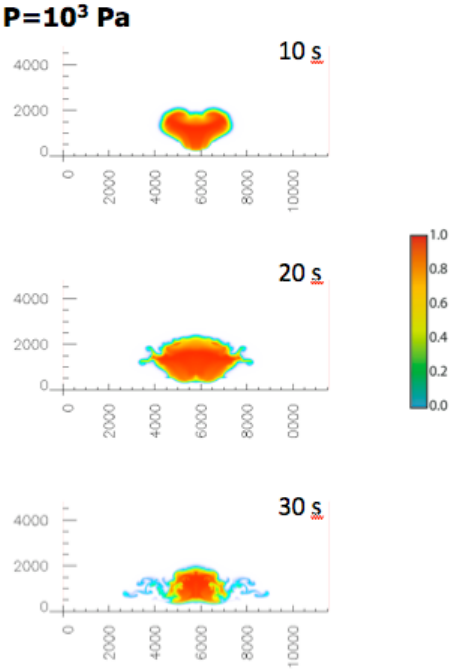

Figure 3. A time sequence of mass fraction of water vapor. Much of the blast region is saturated and accretionary lapilli formation is expected at the margins of the blast were abundant low energy collisions occur.

References: [1]Dufek, J. & Bergantz, G. W. (2007). *J. Theoretical and Computational Fluid Dynamics* 21, 119-145. [2]Clarke, A. B. et al. (2002). *Nature* 415, 897-901. [3]Dartevelle, S. et al. (2004). *Geochemistry Geophysics Geosystems* 5, 1-36. [4]Neri, A. et al. (2007). *GRL* 34, Art. No. L04309. [5]Valentine, G. A. & Wohletz, K. H. (1989). *JGR* 94, 1867-1887. [6]Dufek, J. D. & Bergantz, G. W. (2005). *JVGR* 143, 113-132. [7]Jackson, R. in Theory of Dispersed Multiphase Flow (ed. Meyer, R. E.) (Academic Press, Inc, New York, NY, 1983). [8]Lun, C. K. K. et al. (1984). *JFM* 140, 223-256. [9]Syamlal, M. (National Technical Information Service, Springfield, VA, 1987). [10]Namiki, A. & Manga, M. (2005). *EPSL* 236, 269-284. [11]Rowland, J. C. in Department of Earth and Planetary Science 176 (University of California, Berkeley, 2007). [12]Ross, P. S. et al. (2008). *JVGR* 178, 104-112. [13]Telling, J. & Dufek, J. in AGU Fall Meeting (San Francisco, CA, 2010).